Proceedings of the 2018 ASME International Conference and Exposition on Noise Control Engineering
NCAD2018
August 26-29, 2018, Chicago, IL, USA

NCAD2018-6103

SOUND ATTENUATION IN A FLOW DUCT PERIODICALLY LOADED WITH MICRO-PERFORATED PATCHES BACKED BY HELMHOLTZ RESONATORS

T. Bravo
Instituto de Tecnologias Fisicas y de la Informacion
Consejo Superior de Investigaciones Cientificas
Madrid, Spain

C. Maury
Laboratory of Mechanics and Acoustics - CNRS
Ecole Centrale Marseille
Marseille, France

ABSTRACT

Mitigating the propagation of low frequency noise sources in ducted flows represents a challenging task since wall treatments have often a limited area and thickness. Loading the periphery of a duct with a periodic distribution of side-branch Helmholtz resonators broadens the bandwidth of the noise attenuated with respect to a single resonator and generates stop bands that inhibit wave propagation. However, significant flow pressure drop may occur along the duct axis that could be reduced using micro-perforated patches at the duct-neck junctions. In this study, a transfer matrix formulation is derived to determine the sound attenuation properties of a periodic distribution of MPPs backed by Helmholtz resonators along the walls of a duct in the plane wave regime. In the no-flow case, it is shown that an optimal choice of the MPP parameters and resonators separation distance lowers the frequencies of maximal attenuation while maintaining broad stopping bands. As observed in the no-flow and low-speed flow cases, these frequencies can be further decreased by coiling the acoustic path length in the resonators cavity, albeit at the expense of narrower bands of low pressure transmission. The achieved effective wall impedances are compared against Cremer optimal impedance at the first attenuation peak.

INTRODUCTION

The attenuation of the acoustic pressure field in ducted geometries is still a challenging task when addressing the control of low frequency components. This frequency range is present in most of the problems concerned by the aeronautic and building industries. Low-frequency noise content induced by turbulent flow in heating, ventilation and air conditioning system is a classical but unsolved control problem, especially in the low frequency range. Cylindrical expansion chambers have constituted a recurrent solution when shielded by perforated panels and including or not fibrous absorptive materials [1]. The use of classical fibrous material does not represent an option in the presence of an axial flow due to the transport of airborne particles in the working environment and life-cycle limitations. Such systems can be clogged by dust or oily substances which prevent their use in hospitals, food and pharmaceutical industries due to the risks of bacterial contamination. They can also be easily damaged by high flow velocity and temperature conditions, sources of fire hazards, so that they are difficult to use as such to attenuate the intake and exhaust noise of engines and blowers.

The use of side-branch Helmholtz Resonators (HRs) is another option that provides axial damping to waves propagating in a duct. These control devices have been widely used as they are able to provide important attenuation values but confined in a narrow frequency band [2]. To enhance the frequency range of maximum performance, arrangements made up of a set of side-branch HRs combined in different ways has attracted the attention of several authors. One of the first reported works [3] considered an analytical formulation for describing the sound transmission in a duct lined with an array of resonators. They have been modeled using lumped impedance formulation, assuming one-dimensional plane wave propagation and neglecting flow effects. Recommendations have been provided on the relation between the length of the HR openings and the frequency range over which the silencer is active, as well as the influence of ordering dissimilar resonators on the transmission loss (TL). The same problem has been revisited later on [4] with a deeper analysis relating the simulation results with the physical phenomena involved for the wave propagation in periodic waveguides. It has been shown that the solutions that describe the dynamics of periodic systems like a periodic array of scattering sections in a waveguide are Bloch wave functions determined by an

eigenvalue problem of the transfer operator. From the dispersion relation, the Bloch wave number is found to exhibit a band structure, which is investigated in terms of characteristics of the eigenvalue problem.

This approach has also been used for the attenuation of acoustic waves propagating in a train tunnel before shock formation [5] with an array of identical equally spaced HRs connected axially to the main duct tunnel. The authors verified that the Bloch waves are characterized by the emergence of “stopping bands” where the sound waves are quickly damped along the duct axis, and “passing bands” where they can propagate. The stopping bands appear because of the coincidence between the HR resonance and the Bragg reflection due to their periodic arrangements. They occur when the axial spacing between the neighboring resonators becomes a multiple of half the acoustic wavelength.

More recently, the same combination of side-branch resonators mounted in a duct without flow has been explored both theoretically and experimentally [6]. In order to enhance the attenuation bandwidth in the low to medium frequency range, it is necessary not to place the resonators in close proximity to avoid interaction between them that would lead to a decrease of their overall performance. Using the transfer matrix method for simulating the TL properties of a periodic array of HRs, the authors in [6] considered HRs separated by a distance much larger than the resonators dimensions. They validated their prediction against measurements performed on an array of five identical HRs mounted on a duct with one loudspeaker on a side and multiple loads on the other side. Although the averaged TL performance was much improved in relation to those of a single HR, the total dimensions of the resonators were still quite large when considering shifting the maximum attenuation performance to lower frequencies.

Inspired by these results, the authors [7] proposed a periodic configuration of HRs with special attention to obtain good attenuation performance in the low frequency range while maintaining a reasonable size of the device in order to be used in real-life problems. One possible way to achieve these conflicting objectives is to increase the effective path length taken by the acoustic wave when entering into the HR. This idea has been already presented [8] within the frame of acoustic metasurfaces conceived to enhance normal incidence sound absorption at low frequencies. They have presented analytical simulations comparing a classical partition composed of a perforated plate backed by an air cavity, and a metasurface with a coiled air chamber cell backing each aperture of the plate. By this approach, the effective path length of the inner channels within each cell could be made much greater than the thickness of the backing cavity, maintained at a reasonable size. The analytical results showed that total sound absorption could be achieved at 125 Hz with an overall partition depth only equal to 12.2 mm. Even though these results are remarkable, they also present drawbacks, as the frequency range of high absorption is extremely narrow around the target frequency, decreasing rapidly when moving apart from the Helmholtz resonance. Recently, the authors [7] have explored a combination of the previous techniques applied to duct acoustics in order to achieve both high attenuation performance in the low frequency range and over a broad frequency band. To keep a reasonable size for the control device, it was found that a periodic array of side-branch HRs with a coiled back space in the cavity provided a lower frequency for the maximum attenuation and the creation of stop-bands over a broad frequency range. The influence of several physical parameters, including the spatial HR period, the number of resonators and the number of turns in the coiled cavity have been assessed, showing the potential of the proposed methodology for low frequency noise control.

The proposed set-up has been analyzed in the no-flow case and in the presence of a mean axial flow. However, when an airflow is produced by connecting a fan to the pipe, non-acoustical factors also have to be considered. The input pressure to the system must overcome the pressure drop of air with sufficient momentum so that a given airflow rate can be distributed in the conditioned space [9]. The total pressure can be calculated using the modified equation of Bernoulli for rotational, steady and incompressible flows [10]. In case of an airflow passing through a duct, pressure drops appear due to fluid friction or changes in either the direction or the amplitude of the flow velocity, as it occurs when introducing connectors between sections, bands and fittings. These losses depend on the flow rate and on the aspect ratio between the two sections that are connected. Exact evaluation of the dynamic pressure drop is quite complex and, in most cases, is obtained from empirical laws, with a term proportional to the velocity head multiplied by the dynamic loss coefficient, determined experimentally. In the present work, pressure drops are induced by the connection of a resonator neck to the main duct and can be analyzed considering the formulation for a branch take-off, used in air conditioning ducts for splitting the airflow into branches [10]. These connections are responsible of important pressure drops that have to be avoided in practice.

In this work, we propose to complete the previous array of HRs by including Micro-Perforated Panels (MPPs) or patches at the neck-duct junction to limit the pressure drops. MPPs have been widely studied [11,12]. In building acoustics, MPP resonance absorbers consist of panels perforated with holes of sub-millimeter diameter, situated in front of a rigid or flexible backing wall. They dissipate the acoustic energy through viscous losses around the Helmholtz resonance. The use of micro-perforations for reactive and dissipative duct silencers has recently been investigated. It has been found that micro-perforated cylindrical liners constitute efficient sound-attenuating devices without the introduction of porous material [13,14,15]. The problem of limiting pressure drops has been considered in the frame of the aerodynamic drag due to a flow over external acoustic liners used for the control of noise emissions by aircraft propulsion systems [16]. These authors have considered different types of perforate-over-honeycomb liners with various aperture geometries when subjected to a

mean flow in an impedance tube. The axial static pressure drop along the liners was computed based on the liner resistance factor in the frequency range between 400 and 3000 Hz. They have shown that reducing the hole diameter resulted in a reduction of the drag for a typical liner design and studied how the change in the perforate geometry and orientation relative to the flow would create a configuration with improved drag performance. Measurements were carried out at Mach $M = 0.3$ and $M = 0.5$ under acoustic tonal excitations. It was concluded that differences in the overall attenuation between the geometries were small and that the acoustic liner performance need not to be sacrificed to reduce the liner drag.

Following these results, we propose to insert MPP patches at the entrance of side-branch HR arrays and quantify their effects on the TL performance. The aim is to compare the effective impedance of the HR array against optimal impedance models [17,18,19] to obtain guidelines on selection and optimization of the main MPP and HR parameters. The contents of the paper are as follows. Sect. 2 presents the HR array configuration and the analytical model implemented to determine the TL under different physical conditions (an air or a coiled cavity, visco-thermal losses and a grazing flow). Results from this model are presented in Sect. 3 in a parametric study to examine how HR arrays with MPP patches, with a coiled cavity and under a uniform mean flow may achieve an optimum wall impedance. Finally, the main conclusions and future works are summarized in the last section.

ANALYTICAL MODEL FOR THE RESONATORS ARRAY

The physical set-up of the problem under study is depicted in Figure 1. It consists of a semi-infinite duct excited by an acoustic source located on one side, and with a semi-anechoic termination on the other side. The influence of a grazing mean flow along the axial direction of the duct is accounted for. In order to attenuate the incident wave, one considers a set of N side-branch HRs, separated by a distance D and connected to the waveguide through a series of MPP patches situated at the HR neck entrance, as indicated in the figure below.

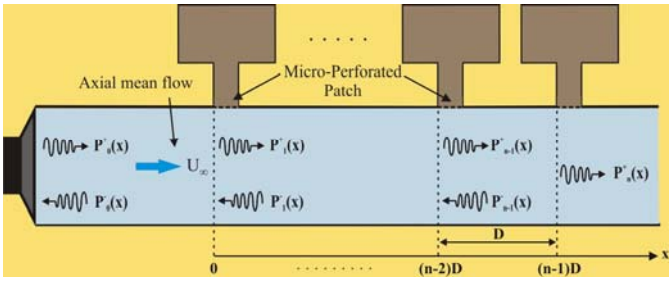

Figure 1. Physical arrangement of an array of HRs connected by MPP patches to a straight duct carrying a mean axial flow and subjected to an acoustic excitation.

To obtain analytical expressions to predict the TL of the complete system, we start by summarizing the main impedance equations that describe the resistive and reactive behavior of a single HR in terms of the resonator physical constitutive parameters. This leads to a transfer model for a periodic array of HRs plugged with MPP patches onto a rectangular duct that constitutes the whole control system.

Input impedance for the basic HR cell with MPP

The classical model for a single resonator unit with MPP expresses the input impedance at the entrance of the HR as the contribution of three different terms, as follows

$$Z_b = \frac{Z_{\mathrm{MPP}}}{\sigma} + Z_{p1} - \mathrm{i}\frac{S_1}{S_p} Z_0 \cot(k_0 D_1). \qquad (1)$$

The first element, Z_{MPP}/σ, describes the MPP overall transfer impedance. For a rigid MPP with circular holes of diameter d_h and thickness t_h, it is given by the following expression based on short tubes Rayleigh theory [11, 14]

$$\frac{Z_{\mathrm{MPP}}}{\sigma} = \frac{\mathrm{i}\omega\rho_0 t_h}{\sigma}\left[1 - \frac{2}{k_h\sqrt{-\mathrm{i}}}\frac{J_1\left(k_h\sqrt{-\mathrm{i}}\right)}{J_0\left(k_h\sqrt{-\mathrm{i}}\right)}\right]^{-1}, \qquad (2)$$
$$+\frac{\mathrm{i}\omega\rho_0}{\sigma}\frac{8d_h}{3\pi}F_M + \frac{4R_e}{\sigma} + \frac{K|M|}{\sigma}Z_0$$

with σ the perforation ratio, η the dynamic viscosity of the air, $k_h = (d_h/2)/r_{\mathrm{visc.}}(\omega)$, the perforate constant, e.g. the ratio of the hole radius to the viscous boundary layer thickness, $r_{\mathrm{visc.}}(\omega) = \sqrt{\eta/\rho_0\omega}$, and ρ_0 the air density. The first term in Eq. (2) represents the internal part of the transfer impedance while the second and third terms account for added mass and frictional loss end-corrections respectively in the reactance and the resistance, with $R_e = \sqrt{\eta\rho_0\omega/2}$ for holes with rounded edges. This expression includes the flow reactance and resistance corrections that have been educed from flow duct measurements over micro-perforates at Mach $|M| \le 0.15$ [14]. They appear respectively in the second and fourth terms, with $F_M = (1+12.6|M|)^{-3}$ and $K = 0.15$.

In Eq. (1), the second element, Z_{p1}, represents the transfer impedance of the hole neck, that can be described using Maa's model [11] for a single perforation of diameter d_1 and thickness t_1, as

$$Z_{p1} = \mathrm{i}\omega\rho_0 t_1\left[1 - \frac{2}{k_1\sqrt{-\mathrm{i}}}\frac{J_1\left(k_1\sqrt{-\mathrm{i}}\right)}{J_0\left(k_1\sqrt{-\mathrm{i}}\right)}\right]^{-1}, \qquad (3)$$
$$+\mathrm{C}\sqrt{2}\eta\frac{k_1}{d_1} + \mathrm{j}0.85\omega\rho_0 d_1$$

This expression is similar to Eq. (2) except that the terms related with the mean flow are not taken into account and it concerns a single aperture. The correction term, C, takes the value $\mathrm{C}=8$ for a sharp-edged hole and $\mathrm{C}=4$ for a rounded-edged hole that produces less dissipation [14].

Finally, the third element of Eq. (1) is the input impedance of the HR cavity of depth D_1, that can be expressed in a classical form as $-\mathrm{i}\,S_1 Z_0 \cot(k_0 D_1)/S_p$, in terms of S_1 and S_p that are respectively the cross-sections of the neck and of the backing cavity, with $Z_0=\rho_0 c_0$ the air characteristic impedance.

Side-branch resonators array

The individual HRs are connected to a rigid duct of cross-section S_d through the MPP patches. These unit cells are repeated periodically with a separation distance equal to D, as indicated in Figure 1. One also assumes that $D+d_1\approx D$. This system has been analyzed in [6] under no-flow conditions considering multi-dimensional wave propagation in the neck-cavity interface. Here, we consider only plane wave propagation in all the sub-systems, limiting the frequency of analysis below the cut-on frequency of the duct, neck and cavity.

For a particular n^{th} unit cell, the right-going and left-going waves can be expressed as a function of the corresponding pressure amplitudes, as

$$\begin{aligned} P_n^+(x) &= C_n^+ e^{-\mathrm{i}k_0[x-(n-1)D]} \\ P_n^-(x) &= C_n^- e^{\mathrm{i}k_0[x-(n-1)D]} \end{aligned}, \qquad (4)$$

for $(n-1)D\le x\le nD$. At the junction, $x=nD$, continuity conditions are applied for the pressure and for the acoustic flow rate. A linear system of two equations is obtained

$$\begin{aligned} &C_{n+1}^+ + C_{n+1}^- = C_n^+ e^{-\mathrm{i}k_0 D} + C_n^- e^{\mathrm{i}k_0 D} \\ &C_{n+1}^+\left(1+\frac{S_1\rho_0 c_0}{S_d Z_d}\right) - C_{n+1}^-\left(1-\frac{S_1\rho_0 c_0}{S_d Z_d}\right) = \\ &\qquad = C_n^+ e^{-\mathrm{i}k_0 D} - C_n^- e^{\mathrm{i}k_0 D}, \end{aligned} \qquad (5)$$

that is solved for C_{n+1}^+ and C_{n+1}^- as follows,

$$\begin{aligned} C_{n+1}^+ &= C_n^+ e^{-\mathrm{i}k_0 D}\left(1-\frac{S_1\rho_0 c_0}{2S_d Z_d}\right) - C_n^- e^{\mathrm{i}k_0 D}\,\frac{S_1\rho_0 c_0}{2S_d Z_d} \\ C_{n+1}^- &= C_n^+ e^{-\mathrm{i}k_0 D}\,\frac{S_1\rho_0 c_0}{2S_d Z_d} + C_n^- e^{\mathrm{i}k_0 D}\left(1+\frac{S_1\rho_0 c_0}{2S_d Z_d}\right), \end{aligned} \qquad (6)$$

which can be written in matrix form as

$$\begin{bmatrix} C_{n+1}^+ \\ C_{n+1}^- \end{bmatrix} = \mathbf{T}\begin{bmatrix} C_n^+ \\ C_n^- \end{bmatrix} \qquad (7)$$

with

$$\mathbf{T} = \begin{bmatrix} \left(1-\frac{S_1\rho_0 c_0}{2S_d Z_b}\right)e^{-\mathrm{i}k_0 D} & -\frac{1}{2}\frac{S_1\rho_0 c_0}{S_d Z_b}e^{\mathrm{i}k_0 D} \\ \frac{1}{2}\frac{S_1\rho_0 c_0}{S_d Z_b}e^{-\mathrm{i}k_0 D} & \left(1+\frac{S_1\rho_0 c_0}{2S_d Z_b}\right)e^{\mathrm{i}k_0 D} \end{bmatrix} \qquad (8)$$

the transfer matrix of the unit cell, in accordance with [6].

If we consider now an array of N resonators, the total transfer matrix can be calculated as the product of the individual transfer matrices as

$$\mathbf{T}_N = \prod_{i=1}^{N}\mathbf{T}_i = \mathbf{T}^N \qquad (9)$$

where we should consider that $\mathbf{T}_i=\mathbf{T}$ since the resonators are identical.

We can particularize this general theory to the case where we deal with a semi-infinite duct with an anechoic termination on the right-hand side after the last resonator. In this case, there are no waves reflected backwards by the termination and the last reflection coefficient reads $C_N^-=0$. Assuming also a unit incident plane wave, $C_0^+=1$ and operating between the previous expressions, Eq. (7) yields the following expression for the transmitted amplitude,

$$C_N^+ = t_{11}^N - \frac{t_{21}^N}{t_{22}^N}t_{12}^N. \qquad (10)$$

The TL for the semi-infinite duct is then given by

$$\mathrm{TL} = 20\log_{10}\left|\frac{C_0^+}{C_N^+}\right| = -20\log_{10}\left|C_N^+\right|, \qquad (11)$$

that will be used in the next section to evaluate the periodic array attenuation performance.

Coiled coplanar air chamber with visco-thermal losses

The air cavity chamber used in classical HRs with or without MPPs can be modified with the objective to increase the total length of the acoustic path and to decrease the HR Helmholtz resonance frequency. For simplicity, we consider a cylindrical neck and a square cavity so that the neck and cavity cross-sectional areas are expressed as $S_1=\pi d_1^2/4$ and $S_p=a^2$. In the coiled resonator, the cavity depth of the classic resonator D_1 is replaced by D_{1c}, the effective length path of the acoustic wave. Assuming p turns in a rectangular folded pattern with quarter-circle path at each bend, the total effective acoustic path length reads

$$D_{1c} = (2p-1)\pi\, w/2 + b + 2(p-1)a, \qquad (12)$$

provided that $2p(w+b) = a$ with w the separation distance between two inner walls and b the walls thickness.

Viscous losses may occur between the walls of the labyrinth, whose separation distance w might be less than twice the viscous boundary layer thickness $r_{\text{visc.}}(\omega)$. This adds further dissipation to the losses already accounted for by the model of Maa in the neck through Eq. (3) and in the MPP patch through Eq. (2). The terms Z_0 and k_0 in Eq. (3) are then replaced by Z_{loss} and k_{loss}

$$Z_{\text{loss}} = Z_0\left[1 - \frac{(1-\mathrm{i})}{\sqrt{2}}\frac{C_{\text{friction}}}{\omega/2}\sqrt{\frac{\eta}{\rho_0\omega}}\right], \qquad (13)$$

$$k_{\text{loss}} = k_0\left[1 - \frac{(1-\mathrm{i})}{\sqrt{2}}\frac{C_{\text{friction}}}{\omega/2}\sqrt{\frac{\eta}{\rho_0\omega}}\right], \qquad (14)$$

where the friction coefficient, $C_{\text{friction}} = 1.47$, is calculated as $C_{\text{friction}} = 1 + (\gamma - 1)/\sqrt{p_r}$. $\gamma = c_p/c_V = 1.4$ is the ratio of the air specific heat at constant pressure and volume respectively, $p_r = \eta c_p/\kappa_T = 0.72$ is the Prandtl number and κ_T is the air thermal conductivity.

Side-branch resonators array

Periodic systems like the one under study have already been analyzed in terms of the Bloch wave theory [4]. They are characterized by the condition

$$f(x+D) = e^{\mu} f(x), \qquad (15)$$

that allows to obtain a recursive relation on the pressure amplitudes relating two consecutive control units as

$$\begin{bmatrix} C_{n+1}^{+} & C_{n+1}^{-} \end{bmatrix}^{\mathrm{T}} = \mathrm{e}^{\mu}\begin{bmatrix} C_{n}^{+} & C_{n}^{-} \end{bmatrix}^{\mathrm{T}}, \qquad (16)$$

with e^{μ} the eigenvalue of the transfer matrix $\mathbf{T}$. The analysis of the characteristic wave solutions is then reduced to the eigen-analysis of $\mathbf{T}$. The eigenvalue e^{μ} determines the propagation of a particular wave type defined by its corresponding eigenvector $\begin{bmatrix} v^{+} & v^{-} \end{bmatrix}^{\mathrm{T}}$ that contains a linear combination of positive and negative-going plane waves. The solutions μ are complex-valued and composed of a real part, μ_r, the attenuation constant, that describes the amount of attenuation experienced by the waves travelling along the duct axis, and an imaginary part, μ_i, the phase constant, responsible of phase changes that can be a pure delay for propagating waves or a π rotation for a HR resonance. Frequency ranges occur in which $\mu_r = 0$ and $\mu_r \neq 0$ denoted pass and stop bands, respectively. In the case of a semi-infinite duct, only the positive-going plane wave exists and Eq. (16) can be simplified to

$$\begin{bmatrix} C_{n}^{+} & C_{n}^{-} \end{bmatrix}^{\mathrm{T}} = a_n \begin{bmatrix} v_1^{+} & v_1^{-} \end{bmatrix}^{\mathrm{T}},\ n = 1,2,\ldots,N. \qquad (17)$$

Considering that the solution of the system can be obtained by the periodic application of the transmission relation (7), the complex constant a_n is expressed as $a_n = a_1\lambda_1^{n-1}$ [6].

PARAMETRIC STUDIES

The averaged TL results obtained from the transfer matrix formulation will be first compared against results published in the literature and then used to assess the influence of several parameters on the TL performance of resonators arrays. In particular, the effect of MPP patches will be examined as well as the resonators separation distance, an elongated coiled acoustic path in the HRs cavity, visco-thermal losses in the HR neck and cavity, and a low-speed uniform flow in the duct. By default, the nominal constitutive parameters of the HRs used in the simulations are as follows: a neck diameter $d_1 = 3.5\,\text{cm}$, a neck length $t_1 = 4.55\,\text{cm}$ connected to a square cavity of depth $D_1 = 4\,\text{cm}$ and of cross-sectional surface area $S_p = 8.33 \times 8.33\,\text{cm}^2$. Each HR is plugged onto the top wall of a rigid rectangular duct of cross-sectional area $S_d = a_d \times b_d = 3.63 \times 3.63\,\text{cm}^2$. MPP patches with holes diameter $d_h = 0.5\,\text{mm}$, thickness $t_h = 0.5\,\text{mm}$ and perforation ratio $\sigma = 8.7\%$, are eventually inserted at the neck-duct junctions. As it can be seen in Figure 1, the duct is excited by an incident plane wave incoming from the left-hand side of the duct and the right-hand side termination is assumed to be anechoic. The array is made up of a periodic distribution of 5 Helmholtz resonators separated from each other by a distance $D = 0.4\,\text{m}$. Simulations have been carried out up to 1 kHz, well below the first cavity, neck and duct cut-on frequencies, respectively at 1810 Hz, 4250 Hz and 4857 Hz. A plane wave regime is assumed in the corresponding fluid domains, including at the neck-cavity interface.

Influence of MPP patches on the TL of resonators arrays

For comparison purposes, these parameters are those used in [6] in which a plane wave regime was assumed in the main duct. In the paper [6], a modal formulation was proposed for the wave propagation in the neck and in the cavity and the averaged TL of an array of HRs without MPP patches was predicted in the no-flow case. It can be seen that the averaged TLs predicted by the present model and corresponding to the black curves in Figure 2

associated to a single HR and an array of 5 HRs without MPP are in excellent agreement with those shown in Figure 8 from [6].

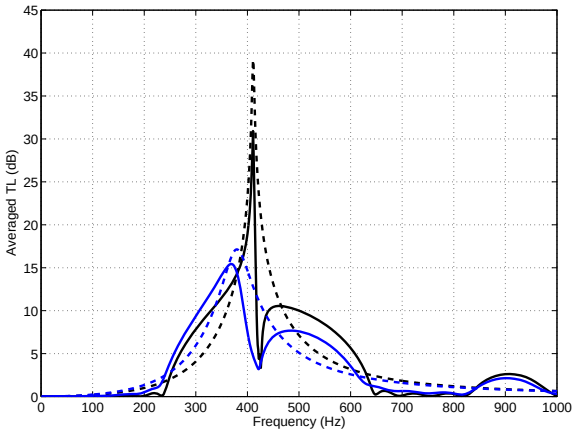

Figure 2. Influence of MPP patches at the duct-neck junction on the averaged TL of side branch resonators made up of a single HR (dashed black: without MPP; dashed blue: with MPP) and an array of $N = 5$ HRs separated by a distance $D = 0.4\,\mathrm{m}$ (solid black: without MPP; solid blue: with MPP).

A major feature due to a periodic array of HRs is to provide extra bandwidths over which the axial attenuation is enhanced with respect to that of a single HR that solely exhibits a sharp and narrow peak around its Helmholtz resonance frequency $f_{\mathrm{H}} = 411\mathrm{Hz}$. Indeed, a periodic array of HRs provides an averaged TL that exceeds that due to a single HR over the bands $248\,\mathrm{Hz} - 380\,\mathrm{Hz}$, $465\,\mathrm{Hz} - 630\,\mathrm{Hz}$ and $843\,\mathrm{Hz} - 982\,\mathrm{Hz}$. Above f_{H}, stop bands appear around the Bragg resonance frequencies, $f_{n,\mathrm{B}}$, that occur whenever the separation distance between two resonators comprises an even or odd number of half-wavelengths, *e.g.* when $k_{n,\mathrm{B}} D = n\pi,\ n \geq 1$ or equivalently when $f_{n,\mathrm{B}} = nc_0/(2D)$. At these frequencies, pressure-release axial resonances occur between two consecutive neck-duct junctions. They block the axial propagation of sound waves, as observed in Figure 2 over the bands $425\,\mathrm{Hz} - 650\,\mathrm{Hz}$ and $820\,\mathrm{Hz} - 1000\,\mathrm{Hz}$.

Inserting MPP patches at the duct-neck junctions adds further resistance and reactance to the input impedance Z_b at the HR entrance, as seen from Eq. (3). As observed from Figure 2 in the case of a single HR, this shifts the Helmholtz resonance frequency from 411 Hz down to 379 Hz. It also lowers the attenuation peak by about 22 dB and broadens its half-bandwidth. If one considers an array of 5 HRs, a similar effect occurs around the first maximum of attenuation with a further shift of the Helmholtz resonance frequency down to 369 Hz and a 15dB reduction of the attenuation peak with respect to a single HR with MPP. However, inserting MPP patches hardly modifies the total bandwidths $200\,\mathrm{Hz} - 630\,\mathrm{Hz}$ and $820\,\mathrm{Hz} - 1000\,\mathrm{Hz}$ within which the incident wave is not fully transmitted, or in other words, it weakly affects the widths of the pass bands.

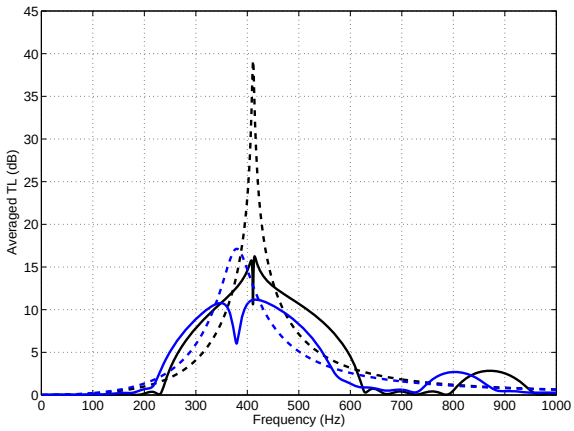

Figure 3. Influence of MPPs on the averaged TL of side branch resonators made up of a single HR (dashed black: without MPP; dashed blue: with MPP) and an optimized array of 5 HRs (solid black: without MPP, $D_{\mathrm{opt}} = 0.42\ \mathrm{m}$; solid blue: with MPP, $D_{\mathrm{opt}}^{\mathrm{MPP}} = 0.45\ \mathrm{m}$).

Figure 3 shows the influence of MPP patches on the averaged TL of HR arrays whose separation distance has been or not optimized. In accordance with [5,20], there exists an optimal separation distance D_{opt} between two consecutive resonators that maximizes the bandwidth of the averaged TL around f_{H}. It is achieved when the Helmholtz frequency coincides with the first Bragg resonance frequency, *e.g.* when $f_{\mathrm{H}} = f_{1,\mathrm{B}} = c_0/(2D_{\mathrm{opt}})$. From Figure 3, it can be seen that increasing the structural periodicity of HRs without (resp. with) MPPs from $D = 0.4\,\mathrm{m}$ to $D_{\mathrm{opt}} = 0.42\ \mathrm{m}$ (resp. $D_{\mathrm{opt}}^{\mathrm{MPP}} = 0.45\ \mathrm{m}$) significantly broadens the half-bandwidth of the first stop band, due to merging between the Helmholtz and the first Bragg resonances. This is achieved at the expense of a reduction in the averaged TL peak value that decreases from 31 dB down to 16 dB for an array of 5 HRs without MPPs. In this case, the first stop band is symmetric with respect to 411 Hz, frequency at which a sharp gap of 5 dB occurs in the averaged TL. When inserting MPPs, this gap in the averaged TL occurs at a lower frequency, 379 Hz. It drops by the same amount, 5 dB, but it is broader and well separates two humps due to strong energy exchange

between the coincident Helmholtz and first Bragg resonant states.

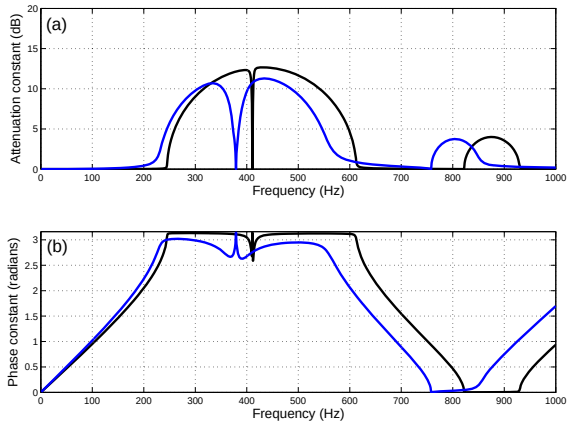

Figure 4. Influence of MPPs (a) on the attenuation constant and (b) on the phase constant of an optimized array composed of an infinite number of HRs (solid black: without MPP, $D_{\text{opt}} = 0.42$ m; solid blue: with MPP, $D_{\text{opt}}^{\text{MPP}} = 0.45$ m).

This doubling resonance feature appears clearly in Figure 4(a) which also shows that the averaged TL tends towards the attenuation constant of the positive-going waves obtained from an eigen-analysis of the elementary cell transfer matrix. Moreover, slight phase variations can be seen in Figure 4(b) over the first stop band of HRs with MPPs whereas the phase is constant (except around the gap) when considering HRs without MPPs. An alternative representation of these effects can be seen in Figure 5.

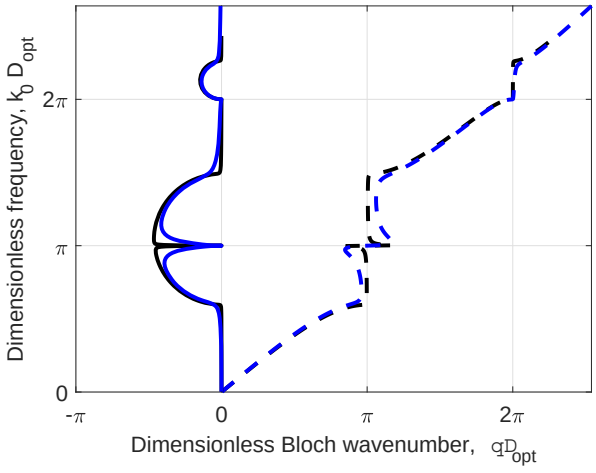

Figure 5. Bloch-Floquet dispersion curves (solid: $-\text{Im}\left(qD_{\text{opt}}\right)$; dashed: $\text{Re}\left(qD_{\text{opt}}\right)$; $q = \text{i}\mu$) for the optimal array of HRs (black: without MPPs; blue: with MPPs).

Bragg stop bands are clearly regognized from the dispersion curves in Figure 5: they occur whenever $\text{Re}\left(qD_{\text{opt}}\right) = \text{cte} = n\pi, n = 1, 2$. Also, The HR separation distance has been optimized such that the first Bragg stop band coincides with the HR resonance frequency. Hence, both resonances occur when $k_{\text{H}} D_{\text{opt}} = \pi = \text{Re}\left(qD_{\text{opt}}\right)$. Mechanisms of energy exchange between the two coupled resonances with or without MPPs are important because they may generate a trough in the first stop band of the averaged TL, as seen in Figure 4(a). This would require further studies to limit this effect.

Influence of a coiled cavity on the TL of resonators arrays

It has been seen that periodic arrays of HRs without MPPs, but with an optimized separation distance, exhibit enhanced attenuation over a broad stop-band in the mid-frequency range. Inserting MPPs at the duct-neck junction lowers the frequency of maximum averaged TL, but it hardly changes the first stop band frequency range. Of interest is to downshift the first stop band without increasing the HRs cavity depth. This can be achieved by increasing the acoustic path length in the cavity in order to lower the Helmholtz resonance frequency f_{H}. Based on the layout proposed in [8] to enhance the performance of resonance absorbers at low frequencies, the acoustic path length in each HR can be extended by inserting a rectangular coil in the cross-sectional plane of the cavity, centred on the axis of the neck opening and whose walls have a height equal to the cavity depth. According to Eq. (12), given the cavity length, width and depth, a target acoustic path length is determined by a suitable choice of the inner walls thickness, b, of their separation distance, w, and of the number of folding turns in the coiled resonator, p, with the constraint that the neck diameter d_1 should stay lower than the wall separation distance, $2w$, in order to avoid obstruction of the neck opening at the junction within the coiled cavity.

Figure 6 shows that a periodic array of 5 coiled HRs with $p = 2$ turns in each cavity, with MPPs and with an optimized spatial period $D_{\text{opt,c}}^{\text{MPP}} = 0.74$ m, downshifts the Helmholtz resonance frequency from $f_{\text{H}}^{\text{MPP}} = 379$ Hz to $f_{\text{H,c}}^{\text{MPP}} = 233$ Hz, reduces the width of the first stop band by a factor 2, but still achieves a broad attenuation between 130 Hz and 350 Hz, with a maximum averaged TL of about 11 dB, almost similar to that of the array of uncoiled HRs. The effective acoustic path length in the resonators is then extended from $D_1 = 0.04$ m to $D_{1,\text{c}} = 0.26$ m.

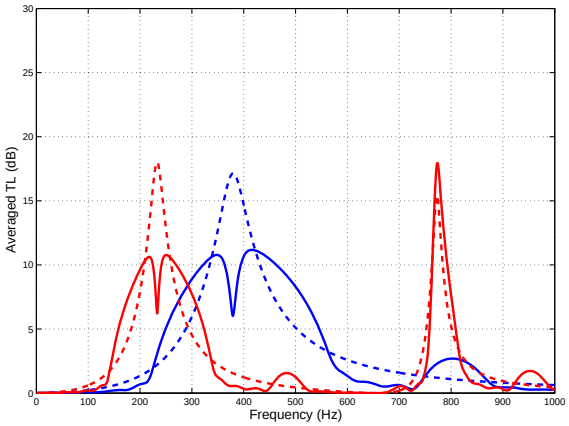

Figure 6. Influence of a coiled cavity on the averaged TL of a single HR with MPPs (dashed curves) and on a periodic network of 5 HRs with MPPs (thick curves) assuming an air cavity (blue curves) and a 2-turn folded acoustic path in the cavity cross-sectional plane (red curves).

One observes in Figure 6 that the network of coiled resonators with MPPs exhibits a sharp and narrow peak of averaged TL that reaches 18 dB at 774 Hz. However, it would reach up to 30 dB without the MPPs dampening effect. This peak is due to the first high-order quarter-wavelength resonance of the HR that, in a first approximation, occurs at $f_{n,1/4,\mathrm{c}} = (2n+1)c_0/\left[4(D_{1,\mathrm{c}} + t_1)\right]$ with $n \geq 1$. The theoretical value, 839 Hz, overestimates by 8% the frequency of peak averaged TL shown in Figure 6. These resonances occur due to the back-cavity cross section of the coiled resonator, $S_{p,\mathrm{c}} = 4w^2$, being only slightly greater than the neck cross-section S_1, so that $S_{p,\mathrm{c}}/S_1 \approx 1.7$ for the array of coiled HRs whereas $S_p/S_1 \approx 7.6$ for the array of uncoiled HRs. Note that $S_{p,\mathrm{c}}/S_1$ tends to 1 as the number of turns in the folded resonator increases, *e.g.* when one aims at lowering $f_{\mathrm{H,c}}^{\mathrm{MPP}}$.

Accounting for visco-thermal losses between the walls of the air cavity and between the walls of the coiled labyrinth is assessed in Figure 7 for a periodic network of 5 HRs with MPPs. With a 2-turn folded resonator, the coil walls are separated by a distance $w = 0.02\,\mathrm{m}$. The visco-thermal losses then hardly affects the averaged TL over the first and higher-order Bragg stop bands, except at 774 Hz, the the first high-order quarter-wavelength resonance, with an averaged TL peak reduced by 5 dB. As expected, the visco-thermal losses can be neglected for the HRs with air cavity.

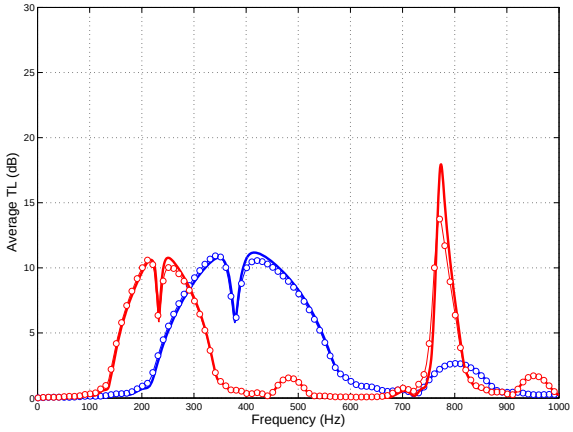

Figure 7. Influence of viscothermal losses on the averaged TL of a periodic network of 5 HRs with MPPs assuming an air cavity (blue curves) or a 2-turn folded acoustic path in the cavity cross-sectional plane (red curves): without losses (thick solid) and with losses (thin solid with circles).

Influence of a uniform flow

Figure 8 shows the effect of a low speed uniform grazing flow on the averaged TL performance of a periodic network of 5 HRs with MPPs at the neck-duct junctions and with either an air or a coiled cavity. Mean-flow effects on the MPP is accounted for through educed reactance and resistance terms that appear respectively as the second and fourth terms in Eq. (2) for the MPP overall transfer impedance. From these expressions, it can be seen that grazing flow increases the MPP resistance by a fraction of the Mach number whereas it decreases the outer end-correction of the MPP holes at the neck-duct opening, but to a lesser extent than the resistance. For a mean flow speed of $17\,\mathrm{ms}^{-1}$ (Mach 0.05), the added flow specific resistance amounts to 0.08 whereas the specific reactance is reduced by a multiplicative factor $F_M = 0.23$.

It can be seen from Figure 8 that the resistance added to the HRs arrays by the low-speed flow causes a decrease by up to 4 dB of the maximum averaged TL at the first stop-band and, for the coiled cavity, at both the first stop-band and quarter-wavelength resonance. Moreover, the grazing flow slightly increases the width of the first stop-band. The flow mass end corrections only provide minute increases of the Helmholtz resonance frequencies of the HRs with air and coiled cavities due to the low flow speed.

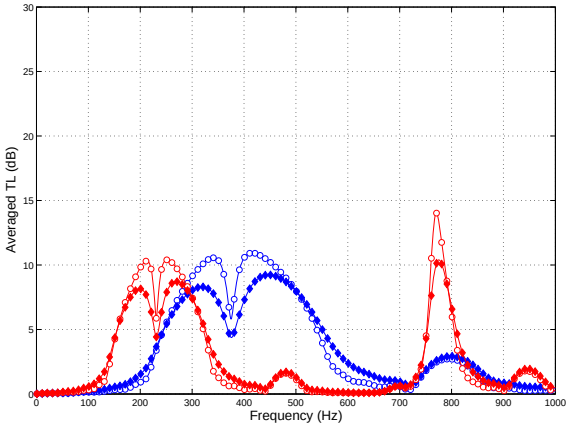

Figure 8. Mean-flow effect on the averaged TL of a periodic network of 5 HRs with MPPs assuming an air cavity (blue curves) and a 2-turn coiled path in the cavity (red curves): without flow (thin solid with circles) and with flow at Mach 0.05 (thin solid with diamonds); losses are accounted for in the cavity.

Comparison against optimal impedance models

It is of interest to determine if the effective impedance of the duct wall onto which is plugged an array made up of a periodic distribution of Helmholtz resonators is close to exact optimal wall impedances that maximize the axial damping of the least attenuated mode, e.g. the plane wave mode. They have been derived by Cremer [17] for a rectangular duct in the no-flow case and more recently in [19] for a circular duct with uniform mean flow, extending the asymptotic results of Tester [18]. In the no-flow case, Cremer [17] showed that the maximum axial decay rate of the least attenuated mode in a rectangular duct of height b_d was achieved for the optimum impedance value, $Z_{\text{opt}} = (0.94 - 0.74\text{i})k_0 b_d / \pi$, of the one-sided locally-reacting wall treatment. In order to compare with this optimal impedance, an effective impedance can be defined for a periodic array of HRs as $Z_{\text{eff}} = Z_{\text{in}} / \sigma_e$ with $\sigma_e = S_1 / (a_d D_{\text{opt}})$ the percentage of open area obtained by dividing the section of the neck, S_1, by the section of the elementary cell $a_d D_{\text{opt}}$. The closest match with the Cremer impedance, $Z_{\text{opt}} = 0.051 - 0.041\text{i}$, evaluated at the first attenuation peak, is obtained at $f_{\text{H,c}} = 256\,\text{Hz}$ for an array of HRs with a coiled cavity and without MPPs for which $Z_{\text{eff,c}} = 0.079 - 0.024\text{i}$. The second closest match is found at $f_{\text{H}} = 411\text{Hz}$ for an array of HRs with an air cavity and without MPPs, for which $Z_{\text{eff}} = 0.069 - 0.007\text{i}$ whereas $Z_{\text{opt}} = 0.082 - 0.064\text{i}$. Inserting MPP patches at the neck-duct junctions brings added resistance that moves the effective impedance, $Z_{\text{eff}}^{\text{MPP}} = 1.082 - 0.039\text{i}$ evaluated at $f_{\text{H}}^{\text{MPP}} = 379\,\text{Hz}$ ($k_0 b_d = 0.25$), further away from the optimal impedance $Z_{\text{opt}} = 0.075 - 0.059\text{i}$. Another added resistance is brought by the visco-thermal losses and by the mean flow effects. For instance, if these two effects are accounted for, one finds $Z_{\text{eff}}^{\text{MPP, flow}} = 2.93 - 0.12\text{i}$ at 379 Hz, the effective impedance for an array of HRs with air cavity and with MPPs in contact with a mean flow of Mach number $M = 0.05$. It is far, especially the resistive part, from the asymptotic optimal impedance $Z_{\text{opt}}^{\text{flow}} = Z_{\text{opt}} / (1+M)^2 = 0.068 - 0.053\text{i}$ derived by Tester [18] and valid for very low Mach numbers. Suitable MPP parameters could then be found so that the effective resistance of the HR array gets closer to the desired optimal resistance. If visco-thermal losses are negligible in the cavity, the optimal reactance can then be achieved through suitable adjustment of the cavity parameters, as carried out in [19] for MPP silencers. If visco-thermal losses cannot be neglected, they may substantially modify the effective reactance and resistance so that both quantities should be simultaneously optimized.

CONCLUSIONS

A transfer matrix formulation has been presented to predict the averaged TL of arrays made up of a periodic distribution of side-branch Helmholtz resonators plugged through MPP patches to a main duct carrying a uniform grazing flow. Such a distribution creates a set of stop bands for which the acoustic wave is attenuated when travelling through each HR cell. Setting the spatial period between the HRs at half the Helmholtz resonance wavelength significantly broadens the width of the first stop band, due to merging between the Helmholtz and the first Bragg resonances. Coiling up the acoustic path in the cross-section of the HRs cavity significantly lowers the stop bands centre frequencies, here by a factor 1.6 for a 2-turns folded path, while still achieving a broad attenuation bandwidth. For the geometry considered, the effect of visco-thermal losses on the attenuation levels over the first stop-band are moderate for classic and 2-turns folded path cavities.

Although HRs with MPPs are keen to limit the flow pressure drop, it was found that inserting MPP patches at the neck-duct junction of periodic HR arrays lowers the maximum attenuation level by up to 5dB and creates doubling resonance phenomenon that breaks the symmetry of the first stop-band and generates a gap in the TL, all the more sharper than the number of HRs increases. As expected, this

feature was still observed when coiling up the HR cavity air space or when accounting for visco-thermal losses in the cavity. It was verified that the added resistance brought by the MPP moves the HR array effective impedance away from Cremer's optimal impedance at the first stop-band centre frequency.

A uniform low-speed flow adds further resistance to the HR array effective impedance, thereby decreasing by up to 4 dB the averaged TL peak with respect to the no-flow case. It corresponds to the worst configuration in which the effective resistance is the furthest from the optimal one with flow. The closest match with the optimal Cremer impedance was obtained at the first attenuation peak for an array of HRs with a coiled cavity and without MPPs.

Subsequent studies could be driven by the search for suitable MPP and/or HR parameters that would provide an effective impedance of the HR array that would match the wall optimal impedance at the HR Helmholtz resonance in the flow case. Such optimization study is expected to limit the sharp TL trough within the first stop-band.

ACKNOWLEDGMENTS

This work has been funded by The Ministerio de Economía y Competitividad in Spain, project TRA2017-87978-R, AEI/FEDER, UE, “Programa Estatal de Investigación, Desarrollo e Innovación Orientada a los Retos de la Sociedad”, and and by the programme A*MIDEX Excellence Initiative of Aix-Marseille University, a French "Investissements d'Avenir" programme, carried out in the framework of the Labex Mechanics and Complexity AAP2.

REFERENCES

[1] Munjal, M. L., 2013, “Recent advances in muffler acoustics”, International Journal of Acoustics and Vibration, Vol. 18, pp. 71–85.

[2] Ingard U., 2010, “Noise Reduction Analysis”, Jones and Bartlett Publishers, Sudbury, Massachusetts.

[3] Trochidis, A. 1991, “Sound transmission in a duct with an array of lined resonators” Journal of Vibration and Acoustics, Vol. 113, pp. 245–249.

[4] Bradley, C.E., 1994, “Time harmonic acoustic Bloch wave propagation in periodic waveguides. Part I. Theory”, Journal of the Acoustical Society of America, Vol. 96, pp. 1844–1853.

[5] Sugimoto, N., Horioka, T., 1995, “Dispersion characteristics of sound waves in a tunnel with an array of Helmholtz resonators”, Journal of the Acoustical Society of America, Vol. 97, pp. 1446–1459.

[6] Wang, S., Mak, C.M., 2012, “Wave propagation in a duct with a periodic Helmholtz resonator array”, Journal of the Acoustical Society of America, Vol. 131, pp. 1172–1182.

[7] Maury C., Bravo T., 2018, “Sound wave attenuation in a duct with a periodic array of ultrathin Helmholtz resonators”, Proceeding of Euronoise 2018, 27-31 Mai, Crete, Greece, pp. 1-8.

[8] Li, Y., Assouar. B.M., 2016, “Acoustic metasurface-based perfect absorber with deep subwavelength thickness”, Applied Physics Letters, Vol. 108, No. 063502.

[9] Shames, I.H., 2003, “Fluids Mechanisms”, Fourth Edition, McGraw-Hill, New York.

[10] White, F.M., 2011 “Fluids Mechanisms”, Seventh Edition, McGraw-Hill, New York.

[11] Maa, D. Y., 1998, “Potential of microperforated panel absorbers”, Journal of the Acoustical Society of America, Vol. 104, pp. 2861-66.

[12] Maa, D. Y., 1997, “Microperforated-panel wideband absorbers”, Noise Control Engineering Journal, Vol. 29, pp. 77-84.

[13] Guo, Y., Allam S., Åbom, M., 2008, “Micro-perforated Plates for Vehicle Application”, Proceedings of the 37th International Congress and Exhibition on Noise Control Engineering (INTER-NOISE 2008), Shanghai, China, October 2008, pp. 1918–1936.

[14] Allam., S., Åbom, M., 2011, “A New Type of Muffler Based on Microperforated Tubes”, ASME Journal of Vibration and Acoustics, Vol. 133, pp. 1–8.

[15] Bravo T, Maury C, Pinhede C., 2016, “Optimisation of micro-perforated cylindrical silencers in linear and nonlinear regimes”, Journal of Sound and Vibration, Vol. 363, pp. 359-379.

[16] Howerton, B.M, Jones, M.G., 2016, “Acoustic liner drag: measurements on novel facesheet perforate geometries”, Proceedings of the 22 nd AIAA/CEAS Aeroacoustics conference, June 2016, Lyon, France, pp. 1-12.

[17] Cremer, L., 1953, "Theory regarding the attenuation of sound transmitted by air in a rectangular duct with an absorbing wall, and the maximum attenuation constant produced during this process", Acustica, Vol. 3, pp. 249-263. (In German)

[18] Tester, B. J., 1973, “The optimization of modal sound attenuation in ducts, in the absence of mean flow”, Journal of Sound and Vibration, Vol. 27, pp. 477–513.

[19] Zhang, Z., Kabral, K, Nilsson, B., Åbom, M., 2017, “Revisiting the Cremer impedance”, Proceedings of Meetings on Acoustics, Vol. 30, No. 040009, pp. 1–12.

[20] Cai, C., Mak., C.M., 2016, “Noise control zone for a periodic ducted Helmholtz resonator system”, Journal of the Acoustical Society of America, Vol. 14, EL471–477.